Agricultural Systems 153 (2017) 101–108

Contents lists available at ScienceDirect

Agricultural Systems

journal homepage: www.elsevier.com/locate/agsy

Yield comparison of simulated rainfed wheat and barley across Middle-East

Rémy Schoppach [a], Afshin Soltani [b], Thomas R. Sinclair [c,*], Walid Sadok [d]

[a] Earth and Life Institute-Agronomy, Université Catholique de Louvain, Croix du Sud 2, L7.05.14, 1348 Louvain-la-Neuve, Belgium
[b] Agronomy Group, Gorgan University of Agricultural Sciences and Natural Resources, Gorgan 49138-15739, Iran
[c] Department of Crop and Soil Sciences, North Carolina State University, Raleigh, NC 27695-7620, USA
[d] Department of Agronomy and Plant Genetics, University of Minnesota, 411 Borlaug Hall, 1991 Upper Buford Circle, St. Paul, MN 55108, USA

ARTICLE INFO

Article history:
Received 22 October 2016
Received in revised form 13 December 2016
Accepted 28 December 2016
Available online xxxx

Keywords:
Africa
Barley
Drought
Simulation
Wheat
Yield

ABSTRACT

Rain-fed wheat and barley are key crops in the Middle-East. A slight improvement in the effective use of water and in grain yield could greatly improve lives of subsistence farmers. This study aimed to evaluate the relative merits of wheat and barley in this region by simulating yields across 404 uniformly spread locations across 30 growing seasons. The results emphasized the primary importance of sowing date in each location. In comparison to wheat, barley generally was capable of rapid progress through its development stages allowing it to avoid deleterious late-season droughts and to have greater yields in low rainfall regions. A large part of Middle-East appeared unsuited for rain-fed production of these two grain species if seasonal yield variability is a concern.

1. Introduction

The domestication of wheat (*Triticum aestevium*) and barley (*Hordeum vulgare*) took place in the Middle-East and these species have remained key crops for this region. Barley is generally favored over wheat in drier regions because barley is often assumed to have superior yielding ability as compared to wheat under water-limited conditions (Teulat et al., 1997; Wahbi and Sinclair, 2005). Due to economic and socio-cultural factors, wheat is commonly grown in areas where these two crops produce approximately equal yields, but barley remains important especially because of its "high resistance" to salinity and tolerance of poor soils (Kaniewski et al., 2012).

In much of the Middle-East, wheat and barley are grown in rain-fed production systems. For example, in 2008 only 15% of the wheat and 18% of the barley growing areas in the Near East were irrigated (FAO, 2009). These numbers highlight the vital importance of appropriate germplasm to maximize productivity in arid and water-limited regions.

Unfortunately, there are very few references that compare yielding capability between wheat and barley in drought-prone locations. Carvalho et al. (2014) hypothesized that spring barley is better adapted to drought than durum wheat in Mediterranean conditions as a result of a higher root length density in the deep soil profile, but the experimental results did not confirm this hypothesis. This confirmed the results of other authors (Abeledo et al., 2004; Garcia del Moral et al., 1999; Arisnabarreta and Miralles, 2006) and supported the potential significance of these differences in modeling these species (Lafarge and Hammer, 2002; Kemanian et al., 2004). However, the experimental results in comparing wheat and barley are limited to the few locations and growing seasons.

To provide more expansive insight about selecting wheat or barley, simulation analyses using process-based crop models can be used to examine crop development, growth, and yield of each species over a wide range of locations and over a large number of growing seasons (Wahbi and Sinclair, 2005; Lobell and Burke, 2010). Since the late 1980s, separate models for wheat and barley have been constructed and their robustness were confirmed for assessing for each species their development, growth, and yield (Stapper and Harris, 1989; Amir and Sinclair, 1991a, 1991b; Sinclair et al., 1993; Goyne et al., 1993; Jones et al., 2003; Keating et al., 2003; Goyne et al., 1996; Milroy and Goyne, 1995; Hammer et al., 2010; Hoogenboom et al., 2012). However, to allow direct comparisons between simulation results for barley and wheat, it is desirable to use a model with the same structure for both species. In this case, only those variables that define distinguishing developmental traits between species are changed and all other aspects of the models remain identical (Wahbi and Sinclair, 2005).

The overall objective of this study was to use the Simple Simulation Model (SSM) for wheat and barley to compare yields across a grid of 404 locations located uniformly across Middle-East regions and over 30 cropping seasons. The SSM model was adapted from Soltani et al.

* Corresponding author.
E-mail address: trsincla@ncsu.edu (T.R. Sinclair).

http://dx.doi.org/10.1016/j.agsy.2016.12.017
0308-521X/

(2013) to take into account the phenological differences between wheat and barley that have been previously identified (e.g., Wahbi and Sinclair, 2005; Alzuelta et al., 2012). To better reflect the intra-specific variability, five genotypes of each species were used in the simulation to introduce genetic variability in phenological development. Four specific objectives were identified: i) Examine the effect of different sowing dates on wheat and barley yields across all the locations and years, ii) Determine if the use of an accumulated soil water content threshold to determine sowing date can be used to increase crop yield, iii) Compare wheat and barley projected yield performances, both in terms of maximum attainable yield and average yield and iv) Assess risks of occurrence of inadequate yields across growing seasons based on a minimum yield that may be acceptable to a grower.

2. Material and methods

The model used in this study is an updated version of the models developed by Sinclair and co-workers (Amir and Sinclair, 1991a, b; Sinclair and Amir, 1992; Sinclair et al., 1993; Wahbi and Sinclair, 2005; Soltani and Sinclair, 2012), which is now identified as the Simple Simulation Model (SSM) based on the terminology introduced by Soltani and Sinclair (2012). Importantly for the current study, the SSM approach was shown to be robust in simulation of bread wheat in Israel (Amir and Sinclair, 1991a, 1991b) and both wheat and barley in Syria and Lebanon (Wahbi and Sinclair, 2005). More recently the SSM-wheat model was assessed in six field experiments located in the vicinity of Gorgan, Iran during two cropping seasons (Soltani et al., 2013). This model was also compared with three other popular wheat models in respect to robustness and transparency, and the SSM model was found to be equal to or superior to the other three models based on these two criteria (Soltani and Sinclair, 2015).

2.1. Model description

SSM is a mechanistic model that incorporates the processes involved in crop development, growth, and yield formation. It describes key physiological processes to simulate crop response to incident radiation, water availability and nitrogen resources. Leaf area development is based on accumulated temperature, referred to as cumulative temperature units (°C). Daily temperature units are calculated based on a two-linear-segment model with a base temperature (equal to 0 °C for wheat and barley) of zero development, an optimal temperature (depending on genotype) and a critical temperature (equal to 40 °C for the two species) of zero development. The daily temperature used in these calculations is the mean of daily minimum and maximum temperatures. In the model, inadequate water or nitrogen supply decreases daily leaf area development rate and crop growth.

Daily crop growth is dependent on intercepted solar radiation as calculated from crop leaf area index (LAI), multiplied by radiation use efficiency (RUE). For optimum conditions RUE is set to 2.2 g MJ^{-1} photosynthetically active radiation (Wahbi and Sinclair, 2005) for all genotypes and species, but it is adjusted to lower values in SSM depending on temperature and soil water-deficit. Non-optimal soil moisture defined by the fraction of transpirable soil water (FTSW) also results in decreased N accumulation. Therefore, daily mass increase is calculated based on incident radiation, minimum and maximum temperature, LAI, and soil water content. Daily growth is used to update cumulative mass of the crop.

Before seed growth, daily N accumulation is calculated to meet daily demand as a result of increasing leaf area and stem dry matter. Constant values of N concentration in leaves and stems are used as targets when N uptake is not limited. Maximum daily rate of N accumulation in wheat was set at 0.25 g m^{-2} d^{-1} (Sinclair and Amir, 1992; Soltani and Sinclair, 2012) and the actual rate of accumulation is limited to this value even if the demand is higher. In these simulations, it was assumed that there was sufficient N in the soil to meet the daily N uptake.

At times when inadequate soil water resulted in N accumulation rate that did not fully meet the plant demand, the concentration of stem N is allowed to decrease to a minimum of 5 mg g^{-1} (Soltani et al., 2013). Under more severe N uptake limitation, leaf area development is inhibited and the stem can continue to grow at a minimum N concentration. Under extreme N limitation, leaf area development is set equal to zero and N can be remobilized by leaf senescence. As soon as the crop reaches the beginning of seed growth, seeds become the prime sinks for N and daily N demand is calculated as the product of seed growth rate and seed N concentration.

An important feature of the SSM model is that daily transpiration rate (TR) is calculated based on the fact that daily TR is very closely linked to daily CO_2 assimilation rate (Sinclair, 1984). This relationship allows TR to be defined by the daily crop growth multiplied by the atmospheric vapor pressure deficit, and divided by a constant, mechanistically defined transpiration coefficient, which is equal to 5.8 Pa for both wheat and barley. TR is calculated every day so that water for transpiration is removed from the soil, along with direct soil evaporation. Calculation of daily soil water status is completed by adding rainfall and snow melt, and removing water lost as run-off and percolation below the root zone. Based on Soltani et al. (2013), the soil profile was composed of five layers to a total depth of 1200 mm and is described in Table 1. Since extensive soil data were not available in the majority of the simulated locations, it was assumed that the soil was generally of the same type across the 404 locations and the volumetric transpirable soil water was set to 0.13 m^3 m^{-3} (Soltani et al., 2013). The daily increase in depth of water extraction is set to be 30 mm per biological day. The extension rate is set to zero before emergence, after beginning of seed growth, when dry matter production is zero, or the soil layer is dry (FTSW = 0). For each crop and genotype, the extraction depth began at 200 mm at plant emergence and the maximum rooting depth was set to 1000 mm.

2.2. Differences in phenology between wheat and barley

The development of the crop is calculated daily as a function of photoperiod and daily mean temperature. This calculation of crop development is based on the biological days (BD) concept, which defines daily progress to complete a phenological event (Soltani and Sinclair, 2012). The actual accumulation of BD on each day is calculated from functions dependent on temperature, vernalization and water-deficit. All these functions are described in Soltani and Sinclair (2012) and all the parameters used are shown in Table 2.

Wheat and barley are very similar crop species but commonly differ in the duration of their phenological stages. Barley is usually a shorter-season species, although some barley genotypes are longer season types and some wheat genotypes are shorter types. In their comparison of wheat and barley, Wahbi and Sinclair (2005) reported that barley in Syria and Lebanon had a 22% shorter time from end of leaf development to anthesis than wheat and a 14% shorter time from anthesis to the end of grain filling than wheat. These differences are reflected in SSM by the duration of individual developmental stages as defined by the BD needed for each development stage. The biological days of each development stage in the simulations for the two species are given in Table 3. All the others parameters were set equal between wheat and barley, except the potential slope of linear increase in harvest index. The increase in harvest index was set equal to 0.014 g g^{-1} $d^{-1}$for wheat and 0.018 g g^{-1} d^{-1} for barley; with the exception of the wheat cultivar Bezostaya set to 0.012 g g^{-1} d^{-1} and barley cultivar Arabic white set to 0.020 g g^{-1} d^{-1} (Soltani et al., 2013; Wahbi and Sinclair, 2005).

Genetic variation among genotypes within a species was also considered in simulating leaf development as defined by phyllochron, which is the biological time needed for each leaf to develop. Five Middle-East genotypes were considered for each species: Zargos, Tarjan, Koohdasht, Shirudi (Soltani et al., 2013) and Bezostaya (Soltani and Hoogenboom, 2007) for bread heat and Arabic white, Beecher,

Table 1
Soil parameters used at all locations for the simulation.
(Soltani et al., 2013).

L[a]	DLY[b]	SAT[c]	DUL[d]	EXT[e]
1	150	0.472	0.264	0.13
2	150	0.478	0.273	0.13
3	300	0.504	0.328	0.13
4	300	0.52	0.364	0.13
5	300	0.523	0.373	0.13

[a] L = soil layer number from the top to the bottom.
[b] DLY = layer thickness (mm).
[c] SAT = volumetric soil water content at saturation ($cm\ cm^{-1}$).
[d] DUL = drained upper limit ($cm\ cm^{-1}$).
[e] EXT = extractable soil water content ($cm\ cm^{-1}$).

Cytris, Rihane S and Swanneck for barley (Wahbi and Sinclair, 2005). For the five wheat genotypes, phyllochron ranged from 91 to 112 °C, while it ranged from 98 to 111 °C for barley (Table 4).

The simulations for wheat included genotype Bezostaya, which is adapted to colder conditions. The optimal temperature for development for this genotype was set equal to 24 °C instead of 27.5 °C used in all other cases. In addition, the following adjustments in parameters were made for this cultivar: nitrogen grain content of 0.015 $g\ g^{-1}$ instead of 0.0213 $g\ g^{-1}$ for the other wheat genotypes, and a coefficient that specifies acceleration or retardation in development in response to water deficit of 0.4 instead of 0.5.

Table 2
Plant input parameters that were common for the two simulated species.

Parameters	Value	Units
A coefficient (exponent) in power relationship between plant leaf area and mainstem node number	2.34	–
Specific leaf area	0.021	$m^2\ g^{-1}$
Fraction of leaf destruction below the critical temperature	0.01	$m^2\ m^{-2}$
Base temperature for dry matter production	0	°C
Lower optimum temperature for dry matter production	15	°C
Upper optimum temperature for dry matter production	22	°C
Ceiling temperature for dry matter production	35	°C
Extinction coefficient for photosynthetically active radiation (PAR)	0.65	–
Partitioning coefficient to leaves during main phase of leaf area development at lower levels of total crop mass	0.6	$g\ g^{-1}$
Partitioning coefficient to leaves during main phase of leaf area development at higher levels of total crop mass	0.3	$g\ g^{-1}$
Partitioning coefficient to leaves from termination leaf growth on mainstem to beginning of seed growth	0.1	$g\ g^{-1}$
Fraction of crop mass at beginning seed growth which is translocatable to grains	0.22	$g\ g^{-1}$
Potential daily increase (growth) in root depth	30	$mm\ d^{-1}$
FTSW threshold when dry matter production starts to decline	0.3	–
FTSW threshold when leaf area development starts to decline	0.4	–
A coefficient that specifies acceleration or retardation of development in response to water deficit	0.5	–
Specific leaf nitrogen in green leaves (target)	1.5	$g\ N\ m^{-2}$
Specific leaf nitrogen in senesced leaves (minimum)	0.4	$g\ N\ m^{-2}$
Stem nitrogen concentration in green stems (target)	0.015	$g\ N\ g^{-1}$
Stem nitrogen concentration in senesced stems (minimum)	0.005	$g\ N\ g^{-1}$
Grain nitrogen concentration	0.0213	$g\ g^{-1}$
Maximum uptake (fixation) rate of nitrogen $g\ N\ m^{-2}\ d^{-1}$	0.25	
Base temperature for development	0	°C
Lower optimum temperature for development	27.5	°C
Ceiling temperature for development	40	°C
Base temperature for vernalization	−1	°C
Lower optimum temperature for vernalization	0	°C
Upper optimum temperature for vernalization	8	°C
Ceiling temperature for vernalization	12	°C

Table 3
Differences in input biological days for each development interval for wheat and barley.

Phenological stages	Wheat[a]	Barley[a]
From sowing to emergence	4.2	4
From emergence to first-tiller	6	4.5
From first-tiller to first-node (stem-elongation)	10.09	8.04
From first-node to booting (ligule of flag leaf visible)	6.8	6
From booting to ear emergence	2.4	1.62
From ear emergence to anthesis	7.6	5.13
From anthesis to physiological maturity	32.8	23.33
From physiological maturity to harvest maturity	8	8

[a] Values expressed in biological days.

2.3. Weather data

Due to variability of the weather from one year to another, evaluation of crop response to the range of conditions under which crops may be grown required simulations over at least 20 cropping seasons at each location (Sinclair et al., 2014). Obtaining the daily weather data required by the model (minimum and maximum temperature, solar radiation and rainfall) for the required number of seasons in this Middle-East region is challenging given that reliable and complete long-term weather datasets are not available. Consequently, weather data were obtained for 30 growing seasons at each location from the weather generator described below.

The National Centers for Environmental Prediction (NCEP) and National Center for Atmospheric Research (NCAR) re-analysis baseline data were used to produce a retroactive record of daily data (Dee et al., 2011; Uppala et al., 2005). The surface grids were analyzed in the Weather Research and Forecasting (WRF) tool to extract daily values for 30 years, from 1979 to 2008, at the centroid of $1° \times 1°$ point grids in each of the regional blocks. Since crop transpiration rate is mainly driven by vapor pressure deficit of the air, a weighted daily vapor pressure deficit for transpiration was calculated by multiplying by 0.75 the daily difference between minimum and maximum vapor pressure (Tanner and Sinclair, 1983).

The major limitations to crop growth in the Middle-East region are the temporal dynamics of the precipitation and temperature environment. Therefore, it was crucial to verify whether the generated patterns of rainfall and temperature distribution reflected the range of conditions for the simulated regions. An independent, comparison analysis was performed for several locations where historical data were available. The records were checked for distribution of precipitation and for maximum and minimum temperature and the simulated values were shown to give the same distribution as the observed data (unpublished results, Ghanem et al., ICARDA, Rabat, Morocco).

2.4. Crop yield simulations

Simulations were initiated in each growing season on 31 August at each location and each growing season. This date was at the end of

Table 4
Phyllochron for each of the studied genotypes.

Species	Genotypes	Phyllochron (°C)
Wheat	Zargos	91
	Tarjan	95
	Koohdasht	100
	Shirudi	112
	Bezostaya	112
Barley	Arabic white	111
	Beecher	111
	Cytris	106
	Rihane S	98
	Swanneck	109

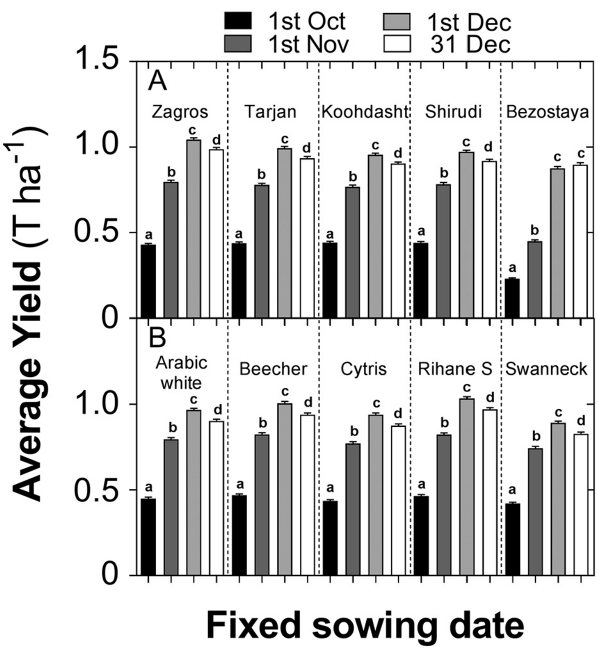

Fig. 1. Genotype-dependent average yield as a function of fixed sowing dates. Ordinate presents the average yield in (T ha^{-1}). Each bar color represents a different fixed sowing date; legend is displayed on the top. Panel A shows the wheat average yields on all the studied locations and all cropping seasons as a function of genotype (±SE) while panel B displays the same results for barley. Genotype names are indicated on the top of the columns. Different letters denote significant statistical differences in average yield inside the genotype category (*t*-tests).

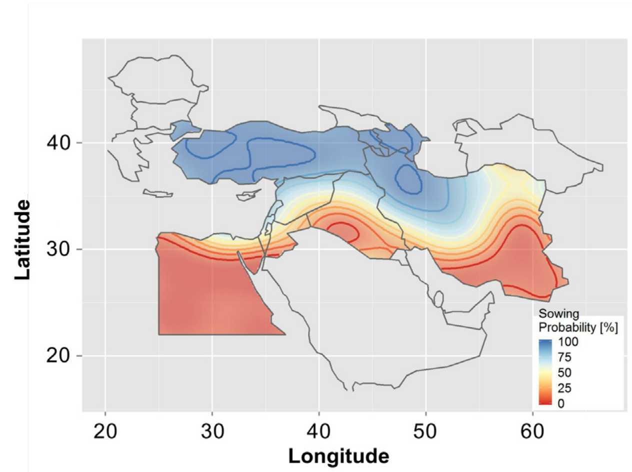

Fig. 3. Simulated sowing probability based on a 15 mm soil water accumulation criterion, within the sowing window for optimum yield. Each area displays the probability of achieving a soil water accumulation threshold of 15 mm during a 30 days window centered on the best sowing date within the four tested. Isometric curves represent equal level-height value from 10% (red) to 100% (dark blue) in increments of 10%. The axes represent latitude and longitude coordinates (in degrees). (For interpretation of the references to color in this figure legend, the reader is referred to the web version of this article.)

the dry season and it was assumed the stored soil water was zero as found in successive simulations. From 31 August until sowing and then plant emergence, soil water status was calculated accounting for daily soil surface evaporation, rainfall, run-off, and deep drainage.

Since this study was to assess yields under rainfed conditions, no irrigation was included in these simulations. The plant density was held constant at 300 plants m^{-2}, which is characteristic in Iran for these crops (Soltani and Hoogenboom, 2007). It was assumed in the simulations that the duration of any cropping season did not extend past August 30 in the year following sowing. So if the simulated crop did not reach maturity before August 30, crop yield was set to the seed mass achieved on that date.

Simulations were done using two approaches to determine sowing date. The first approach was simply to set a fixed day of sowing regardless of the soil water content (Objective 1 of the study). Four fixed sowing dates were simulated: 1 October, 1 November, 1 December, and 31 December. The second approach was to have sowing when soil water content reached a threshold value (Objective 2 of the study). Two thresholds for accumulated water in the soil were tested as criterion for sowing: 15 and 30 mm accumulated soil water content over the entire soil profile. However, no sowing was allowed earlier than 15 d before or later than 15 d after the fixed sowing date out of the four in

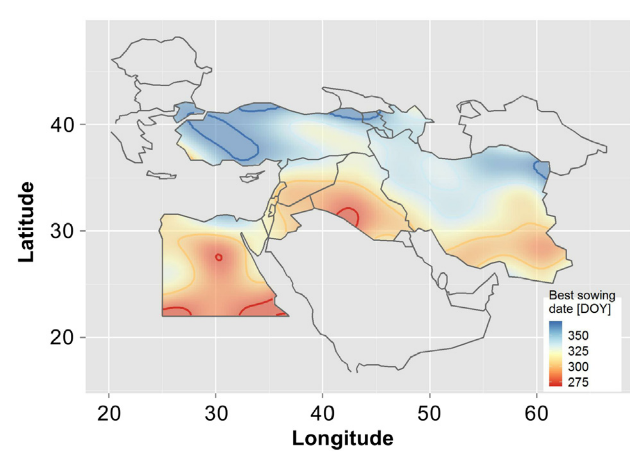

Fig. 2. Kriged map of simulated best sowing date across the Middle-East regions. Spatial representation of the best sowing date resulting in the highest yield for each location based on the highest yielding specie and genotype. Four days of the year (DOY) were tested: 274, 305, 335, 365, corresponding to October 1, November 1, December 1 and December 31 and are represented by isometric curves from red to dark blue respectively. The axes represent latitude and longitude coordinates (in degrees). (For interpretation of the references to color in this figure legend, the reader is referred to the web version of this article.)

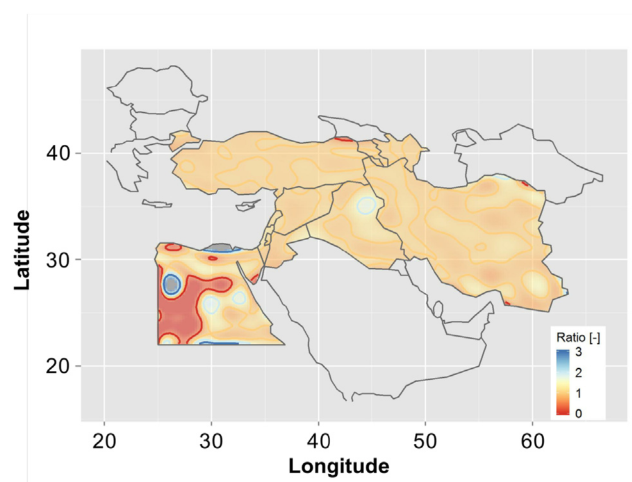

Fig. 4. Ratio of average simulated yield with the sowing based on a 15 mm soil water accumulation criterion divided by simulated yield based on the highest-yielding fixed sowing date. Each area was calculated over the growing seasons achieving the 15 mm soil water accumulation criterion and accounting for the highest yielding species and genotype. Ratio equal to zero represents areas where this criterion was never achieved over the 30 studied growing seasons. Isometric curves represent equal level-height value from 0.5 (red - disadvantage) to 2 (dark blue – advantage) in increments of 0.5. Values below 1 represents yield penalties of 15 mm soil water accumulation criterion while values above 1 represents yield advantage. The axes represent latitude and longitude coordinates (in degrees). (For interpretation of the references to color in this figure legend, the reader is referred to the web version of this article.)

the previous simulations that resulted in the maximum yield. This condition was set to avoid early sowing especially in northern regions where water threshold may be reached early in the season but winter cold could be damaging if crops were sown too early.

2.5. Data analysis software

All simulation results were analyzed using Prism 6.0 (GraphPad Software Inc., San Diego, CA, 2007). The geographical maps were produced using R 3.0.2 (R Core Team, Vienna, Austria, 2013) and the figure constructions were carried out using Prism 6.0.

3. Results and discussion

3.1. Sowing date effects

Objective 1 of this study was to compare the results of four, fixed sowing dates on yield of wheat and barley across 404 locations in the Middle-East and 30 cropping seasons. Fig. 1 shows the mean yield at each location by taking the average of the four sowing dates, all five genotypes, and all 30 seasons including those seasons were no yield was simulated for wheat (Fig. 1A) and barley (Fig. 1B). The range of mean yields based on all results varied from 0.23 to 1.04 T ha^{-1} for wheat and from 0.42 to 1.03 T ha^{-1} for barley, with only small variation attributable to genotypic differences. The greatest source of variation was sowing date with the greatest yields occurring with the 1 December sowing date when mean yields were approximately 1 T ha^{-1}. The single exception to this pattern was the wheat cultivar Bezostaya in which the 31 December sowing had the highest mean yield (Fig. 1A). These exceptional results for Bezostaya were due to the advantage in delayed sowing in Turkey where the highest yields occurred when sowing date was delayed to avoid the cold effect during winter.

The geographical area simulated was quite large and spanned different environmental conditions in terms of patterns and total amount of rainfall and temperature. Plant response to environment, and especially drought, is temporally complex so that traits such as short/long phenological stages are likely to have variable responses across growing seasons and locations. Therefore, it was necessary to do a more refined analysis of the data than just mean yield for each sowing date across the whole area as presented in Fig. 1. Fig. 2 is a map presenting the fixed sowing date at each location that resulted in the highest yielding specie and genotype. Each of the four sowing dates proved to result in maximum yield at some location. December 31 gave the highest yields for much of Turkey and northeast Iran due to avoidance of the cold conditions during winter months and the availability of water during the end of the cropping season (as explemified in Fig. 7B). For east Turkey through much of Iran, the highest yields were achieved with the sowing

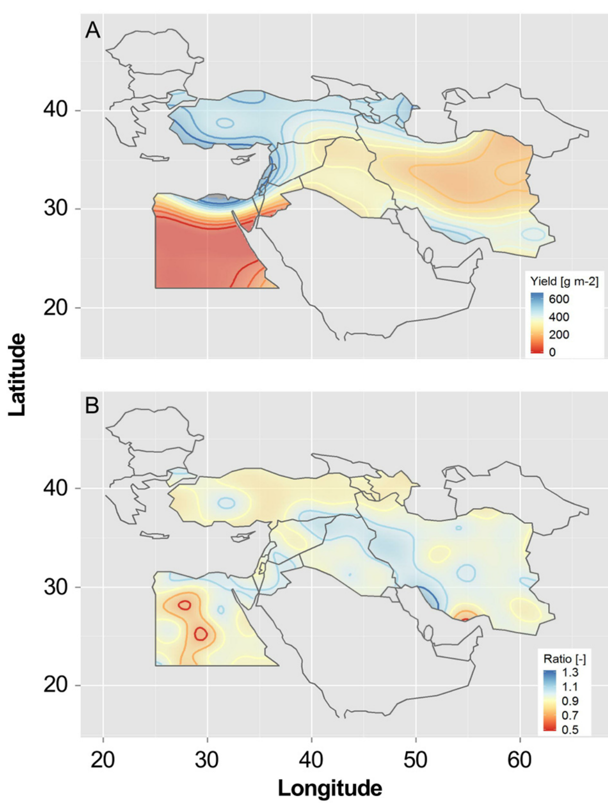

Fig. 5. Wheat simulated maximum attainable yield and comparison with yield of barley. Panel A: Each area represents the maximum attainable yield of wheat based on the highest yielding genotype and sowing date at each location. Barley simulated maximum yield map was almost similar and therefore is not presented. Isometric curves represent equal level-height value from 50 g m^{-2} (red) to 550 g m^{-2} (dark blue) in increments of 50 g m^{-2}. Panel B: Each area represents the ratio of maximum attainable yield for barley divided by maximum attainable yield for wheat, based in both cases on the highest yielding genotype and sowing date. Isometric curves represent equal level-height value from 0.7 (red – advantage for wheat) to 1.1 (dark blue – advantage for barley) in increments of 0.1. Values below 1 represents yield wheat yield advantage while values above 1 represents barley yield advantage. The axes represent latitude and longitude coordinates (in degrees). (For interpretation of the references to color in this figure legend, the reader is referred to the web version of this article.)

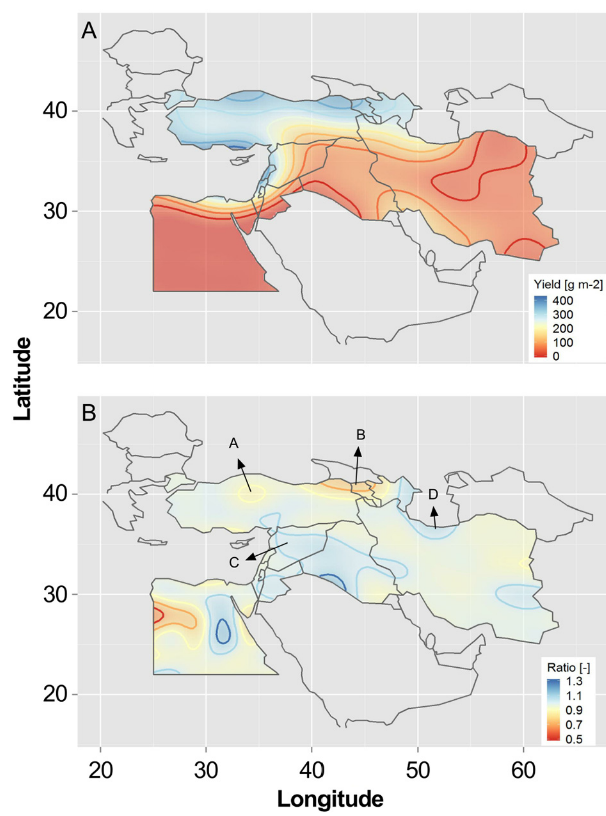

Fig. 6. Wheat simulated average yield and comparison with yield of barley. Panel A: Each area represents the average yield of wheat based on the highest yielding genotype and sowing date at each location, over the 30 studied growing seasons. Barley simulated average yield map was almost similar and therefore is not presented. Isometric curves represent equal level-height value from 50 g m^{-2} (red) to 400 g m^{-2} (dark blue) in increments of 50 g m^{-2}. Panel B: Each area represents the ratio of average yield for barley divided by average yield for wheat, based in both cases on the highest yielding genotype and sowing date. Isometric curves represent equal level-height value from 0.7 (red – advantage for wheat) to 1.1 (dark blue – advantage for barley) in increments of 0.1. Values below 1 represents wheat yield advantage while values above 1 represents barley yield advantage. Black letters from A to D represent locations displayed in Fig. 7. The axes represent latitude and longitude coordinates (in degrees). (For interpretation of the references to color in this figure legend, the reader is referred to the web version of this article.)

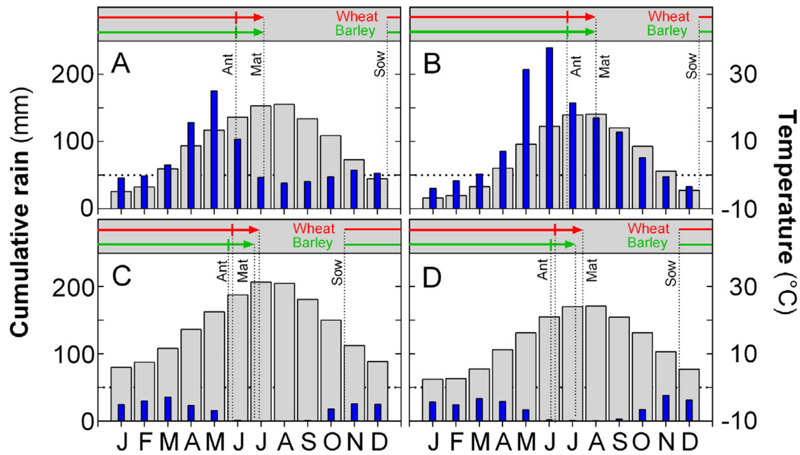

Fig. 7. Monthly average cumulative rainfall and temperature of four contrasted locations across the Middle-East. Each panel letter matches to the letter in Fig. 6B implying that panel from A to D represent respectively areas located at 39.5°–33.5° (latitude-longitude), 40.5°–44.5°, 35.5°–38.5° and 36.5°–51.5°. In each panel, blue bars represent the monthly average cumulative rainfall while the light grey bars represent the monthly average temperature. Time of the year when sowing (Sow), anthesis (Ant) and maturity (Mat) occurred are presented by vertical doted black lines. On the top light grey boxes, wheat and barley growing time from sowing to maturity (arrowhead) are represented by horizontal red and green lines respectively. The small vertical red and green lines represent the time of anthesis. (For interpretation of the references to color in this figure legend, the reader is referred to the web version of this article.)

date of 1 December. The remaining southern drier regions of the simulated area had the highest yields with one of the earlier sowing dates.

The second approach to determining sowing date was to sow when a threshold of accumulated water has been reached in the soil. Such an approach ensured an adequate soil moisture for high germination rate and establishment of the crop. The 15 and 30 mm soil water thresholds produced similar simulated yields, probably because places and years where rainfall were sufficient to reach 15 mm were often equal to or followed within a few days by the accumulation of 30 mm (Schoppach et al., unpublished data). Given these similarities, only data for the 15-mm threshold are discussed.

First, the limitation of achieving 15 mm of soil water within the 30-d sowing window for each location was examined. Somewhat surprisingly, the accumulated-water criterion resulted in a failure to sow in more than half of the simulated land area (Fig. 3). In fact, for many desert regions there was sufficient rainfall to achieve 15 mm of accumulated soil water in <5% of the growing seasons. In contrast to the arid regions, the northern part of the simulated areas showed a high probability of sowing (Fig. 3) and substantial area had sowing in each growing seasons. Additional land area was suitable in meeting the accumulated soil water criterion if it was acceptable for growers to be able to sow in at least 90% of the growing season, i.e. in 10% or fewer seasons there would be insufficient accumulated soil water for sowing.

To explore whether the 15-mm accumulated soil water criterion for sowing was superior to a fixed date for sowing, a ratio was calculated for the average yield simulated using 15-mm sowing criterion and the highest yielding fixed sowing date. Only the growing seasons when the water threshold condition was reached were taken into account in the ratio calculation to ensure a fair comparison. The yield ratios presented in Fig. 4 is for the highest yielding species and genotype at each individual location. Therefore, ratios >1.0 reflected a yield advantage in sowing based on the soil-water accumulation criterion.

The criterion of water accumulation in the soil for sowing did not show an overall clear advantage, i.e. yield ratio > 1.0, in most places of the Middle-East (Fig. 4). In some places like north and west Turkey, there was generally a disadvantage with the accumulated soil water criterion for sowing as compared to using a fixed sowing date. Northwest Iran had a modest yield advantage using the accumulated water threshold as compared to the fixed sowing date (Fig. 4), but again there was no clear trend. The Egyptian regions are very arid and are not actually suitable for wheat or barley production. The yields were so low in these desert regions that ratios varied from advantage to disadvantage for side-by-side locations. Overall, these results showed that advanced or delayed sowing date based on soil water content may only provide slight advantage in some locations but was generally not especially beneficial.

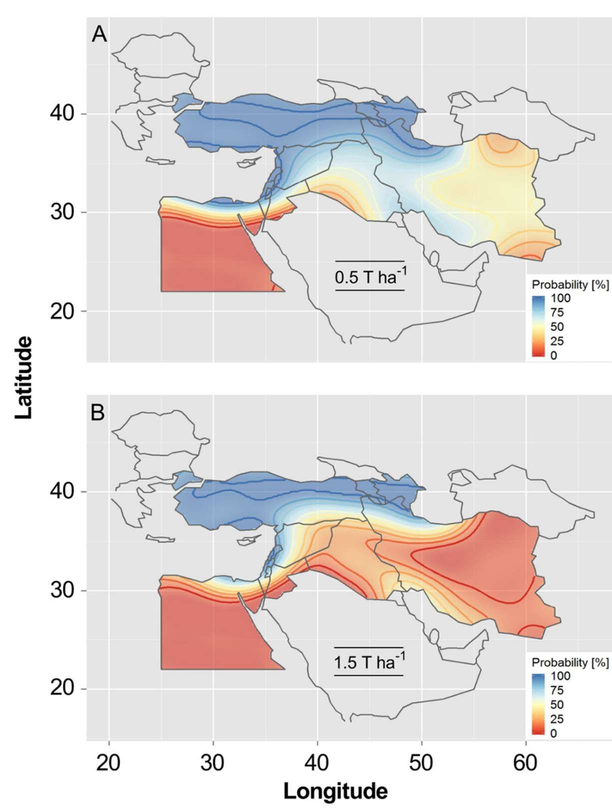

Fig. 8. Growing seasons percentage associated with average yield equal to or greater to 0.5 (panel A) and 1.5 T ha^{-1} (panel B). Each area represents the probability based on the highest yielding specie, genotype and sowing date. Isometric curves represent equal level-height value from 10% (red) to 100% (dark blue) in increments of 10%. The axes represent latitude and longitude coordinates (in degrees). (For interpretation of the references to color in this figure legend, the reader is referred to the web version of this article.)

3.2. Species yield comparison

The relative yield advantage of wheat vs. barley was compared as Objective 3. One basis for assessing the relative advantage of the two species was to compare the maximum yield that might be achieved in each location for the optimal combination of sowing date and genotype for each species. To a considerable extent, the simulated maximum yield maps of wheat and barley (Fig. 5A and B) are similar. Maximum yield ranged from 0 T ha^{-1} in the desert of Egypt to 6.5 T ha^{-1} for wheat (Fig. 5A) in the Nile delta and 6.3 T ha^{-1} for barley (Fig. 5B). Coastal regions always had higher maximum yields than inland regions for both wheat and barley due to greater rainfall. Not surprisingly, there were large, arid areas where the maximum yield for both species was <1.0 T ha^{-1}, and even some locations with much lower yields. Clearly, maximum yield throughout this region is closely linked with precipitation and water availability to support crop development and growth.

Another basis for comparing yield of wheat and barley is the average yield obtained at each location by each species. Average yield was calculated from simulation results for all 30 growing seasons, including those seasons in which zero yield was simulated. The average yield was the mean for the best combination of sowing date and genotype at each location (Fig. 6). The arid, desert regions had little or no yield for both species and included nearly all of Egypt and much of eastern Iran. The highest average yields occurred along the coast of the Mediterranean and Black Seas. For both species, the average in these areas was commonly >3 T ha^{-1}. For wheat as compared to barley, the higher average yields were found further inland from the Black Sea coast and much of Armenia and Azerbaijan. Syria showed a gradient of average yield from 3 to 1 T ha^{-1} from west to east. In Iraq the yield gradient for wheat was 1.0 to 0.5 T ha^{-1} from north to southeast. Iran showed average yield as high as 2.5 T ha^{-1} in the northern regions, and only 1.5 T ha^{-1} along the Persian Gulf.

Temperature and rainfall were key factors in the selection of crop species at each location. This is illustrated by examining four contrasting locations identified by letters in Fig. 6B. Monthly environmental conditions at are presented in detail in Fig. 7. In panels 7A and 7B, the best sowing date at these locations were December 31 for both wheat and barley and the most productive genotypes were Bezostaya and Beecher for wheat and barley, respectively. Simulated anthesis occurred on June 12 for the location in panel 7A and on July 6 for the location in panel 7B for both species. Barley maturity was reached 1 day after wheat for both of these locations, on July 18 and 19, respectively, for location A and August 14 and 15, respectively, for location B. These similarities were due to the lower optimal temperature for development associated with the wheat genotype Bezostaya. While BDs were higher for Bezostaya than barley, its lower base temperature resulted in similar development progress. This situation also explained why the LAI of wheat at anthesis was equal to 4.1 in location A and 3.1 in location B, while the LAI of barley was 2.1 and 1.8 in location A and B, respectively. The higher LAI at anthesis of wheat allowed greater amounts of N for mobilization from leaves to grain during grain filling periods, thereby increased yield. Even if the sowing was delayed to avoid negative effects of winter cold, water availability after anthesis was not a limiting factor in these two locations. The major limiting factor was the cold conditions resulting in less than optimal development of the plants during vegetative phase.

The optimal sowing date at location C (Fig. 7C) was October 1 for both wheat and barley. Simulated anthesis occurred on June 7 for wheat and June 2 for barley, and maturity was reached on July 12 for wheat and July 6 for barley. The wheat genotype displayed a slightly higher LAI at anthesis (2.3 versus 2.0). Despite a lower LAI, the barley crop gave higher yield than wheat since anthesis and maturity occurred earlier in barley than wheat allowing barley to be less affected by late-season drought, which caused major decreases in wheat yield. The sum of water evaporated and transpired during the anthesis-maturity period was 20 mm for wheat and 29 mm for barley reflecting the lower amount of water remaining in the soil at anthesis for wheat.

At location D (Fig. 7D), optimal sowing date was December 1 for both species. Simulated anthesis occurred on June 26 and 21 for wheat and barley, respectively, which resulted in a higher LAI at anthesis for wheat (3.6 vs 2.3). Maturity occurred on July 30 and 22, respectively, for wheat and barley. Like location C, the greater LAI of wheat did not make the wheat more productive than barley because of the water limitation. Water remaining during the grain filling period allowed 26 mm transpiration for barley while the wheat had only 11 mm on average. The major reason resulting in lower wheat yields at locations C and D was the lack of water during the grain-filling period. Not surprisingly, locations with late-season drought have the lowest yields (Wahbi and Sinclair, 2005). If these late drought events are consistent, using a short-season crop appears to be advantageous to avoid yield decrease.

3.3. Risk assessment

An important concept in crop management is the notion of risk. Indeed, subsistence farmers in dry and often poor regions are highly dependent on crop production in every year even if this means overall lower yields, i.e. they are risk adverse. The decision of growing a crop at a certain location may well be based on the probability to attaining at least a minimum yield in a large fraction of cropping seasons rather than a higher average yield. Using the data from these simulations, it was possible to explore the percentage of growing seasons that had yields equal to or greater than various thresholds depending on the expectations of the growers. The results of the simulations were used to explore two yield thresholds: i) 0.5 and ii) 1.5 T ha^{-1}.

The low threshold yield of 0.5 T ha^{-1} was assumed because such a yield would allow a farmer growing grain on 2 ha to produce sufficient calories to sustain a family of six for a year. Fig. 8A shows the probability across the simulated region of achieving this threshold or greater for either wheat or barley. Assuming a very minimum threshold of achieving a yield of 0.5 T ha^{-1} or greater in 60% or more of the growing seasons, large areas are predicted to be unsuitable for rainfed production of either of these cereal species. The whole of Egypt except the Mediterranean coast, the south and east part of Jordan, the east part of Syria and almost all Iraq were predicted to not reach the 0.5 T ha^{-1} threshold in 60% or greater of the growing seasons. Except the northwest, all of Iran was also simulated to be unsuited for rainfed cereal production based on the 0.5 T ha^{-1} threshold.

Alternatively, the 1.5 T ha^{-1} threshold, which may be more appropriate for more intensive agricultural production, showed an even more limited region suited for production of these cereal grains. Only regions above latitude 37.5° N, except more southern, coastal regions, achieved the higher yield threshold. Surprisingly, the area of Iran along the Persian Gulf where the average yield was relatively high (1.5 T ha^{-1}) did not consistently achieve the threshold yield because high variability of rainfall pattern from one year to another.

4. Conclusions

The simulations of wheat and barley using a common model allowed a direct comparison of relative growth, development and yield of the two species across a wide range of 404 locations and 30 simulated growing seasons. The results highlighted the importance of management practices especially optimal sowing date that differed significantly from one region to another. Yields of wheat and barley remained similar as these crop species are very similar except that differences in plant phenology allowed barley to develop more rapidly. Consequently, barley could avoid water-deficit conditions that usually developed during grain filling period in some dry areas. In contrast, in higher rainfall and lower temperature regions, wheat appeared to be more productive due to its ability to grow longer and take advantage of resources during a longer period. The second key conclusion that emerged from this simulation analysis was that the majority of the studied areas are simply not suitable for rain-fed production of these cereal grains because of the high risk of low yield from one season to the next.

Acknowledgment

This research was funded by the Belgian National Fund for Scientific Research (FNRS, contract #1.5108.12) and the FSR fund of the Université catholique de Louvain. Rémy Schoppach is a FRIA (contract #1.E038.13) fellow, Belgium. Walid Sadok was supported by the Minnesota Agricultural Experiment Station (MAES), project MIN-13-095.

References

Abeledo, L.G., Calderinia, D.F., Slafer, G.A., 2004. Leaf appearance, tillering and their coordination in old and modern barleys from Argentina. Field Crop Res. 86, 23–32.
Alzuelta, I., Abeledo, L.G., Mignone, C.M., Miralles, D.J., 2012. Differences between wheat and barley in leaf and tillering coordination under contrasting nitrogen and sulfur conditions. Eur. J. Agron. 41, 92–102.
Amir, J., Sinclair, T.R., 1991a. A model of the temperature and solar radiation effects on spring wheat growth and yield. Field Crop Res. 28, 59–69.
Amir, J., Sinclair, T.R., 1991b. A model of water limitation on spring wheat growth and yield. Field Crop Res. 28, 47–58.
Arisnabarreta, S., Miralles, D.J., 2006. Yield responsiveness in two- and six-rowed barley grown in contrasting nitrogen environments. J. Agron. Crop Sci. 192, 178–185.
Carvalho, P., Azam-Ali, S., Foulkes, M.J., 2014. Quantifying relationships between rooting traits and water uptake under drought in Mediterranean barley and durum wheat. J. Integr. Plant Biol. 56, 455–469.
Dee, D.P., Uppala, S.M., Simmons, J., Berrisford, P., Poli, P., Kobayashi, S., et al., 2011. The ERA-interim reanalysis: configuration and performance of the data assimilation system. Q. J. R. Meteorol. Soc. 137, 553–597.
FAO, 2009. Irrigation in the Middle East region in figures, Aquastat Survey 2008. FAO Water Reports. 34.
Garcia del Moral, L.F., De la Morena, I., Ramos, J.M., 1999. Effects of nitrogen and foliar sulphur interaction on grain yield and yield components in barley. J. Agron. Crop Sci. 72, 176–184.
Goyne, P.J., Milroy, S.P., Lilley, J.M., Hare, J.M., 1993. Radiation interception, radiation use efficiency and growth of barley cultivars. Aust. J. Agric. Res. 44, 1351–1366.
Goyne, P.J., Meinke, H., Milroy, S.P., Hammer, G.L., Hare, J.M., 1996. Development and use of a barley crop simulation model to evaluate production management strategies in north-eastern Australia. Aus. J. Agric. Res. 47, 997–1015.
Hammer, G.L., van Oosterom, E., McLean, G., Chapman, S.C., Broad, I., et al., 2010. Adapting APSIM to model the physiology and genetics of complex adaptive traits in field crops. J. Exp. Bot. 61, 2185–2202.
Hoogenboom, G., Jones, J.W., Wilkens, P.W., Porter, C.H., Boote, K.J., Hunt, L.A., Singh, U., Lizaso, J.L., White, J.W., Uryasev, O., Royce, F.S., Ogoshi, R., Gijsman, A.J., Tsuji, G.Y., Koo, J., 2012. Decision Support System for Agrotechnology Transfer (DSSAT) Version 4.5. University of Hawaii, Honolulu, Hawaii (CD-ROM).
Jones, J.W., Hoogenboom, G., Porter, C.H., Boote, K.J., Batchelor, W.D., Hunt, L.A., Wilkens, P.W., Singh, U., Gijsman, A.J., Ritchie, J.T., 2003. The DSSAT cropping system model. Eur. J. Agron. 18, 235–265.
Kaniewski, D., Van Campo, E., Weiss, H., 2012. Drought is a recurring challenge in the Middle East. Proc. Natl. Acad. Sci. U. S. A. 109, 3862–3867.
Keating, B.A., Carberry, P.S., Hammer, G.L., Probert, M.E., Robertson, M.J., Holzworth, D., Huth, N.I., Hargreaves, J.N.G., Meinke, H., Hochman, Z., McLean, G., Verburg, K., Snow, V., Dimes, J.P., Silburn, M., Wang, E., Brown, S., Bristow, K.L., Asseng, S., Chapman, S., McCown, R.L., Freebairn, D.M., Smith, C.J., 2003. An overview of APSIM, a model designed for farming systems simulation. Eur. J. Agron. 18, 267–288.
Kemanian, A.R., Claudio, O., Stöckle, C.O., Huggins, D.R., 2004. Variability of barley radiation-use efficiency. Crop Sci. 44, 1662–1672.
Lafarge, T.A., Hammer, G.L., 2002. Tillering in grain sorghum over a wide range of population densities: modelling dynamics of tiller fertility. Ann. Bot. 90, 99–110.
Lobell, D.B., Burke, M.B., 2010. On the use of statistical models to predict crop yield responses to climate change. Agric. For. Meteorol. 150, 1443–1452.
Milroy, S.P., Goyne, P.J., 1995. Leaf area development in barley model construction and response to soil moisture status. Aus. J. Agric. Res. 46, 845–860.
R Development Core Team, 2013. R: A Language and Environment for Statistical Computing. R Foundation for Statistical Computing, Vienna. http://www.R-project.org.
Sinclair, T.R., 1984. Leaf area development in field-grown soybeans. Agron. J. 76, 141–146.
Sinclair, T.R., Mosca, G., Bona, S., 1993. Simulation analysis of variation among seasons in winter wheat yields in northern Italy. J. Agron. Crop Sci. 170, 202–207.
Sinclair, T.R., Amir, J., 1992. A model to assess nitrogen limitations on the growth and yield of spring wheat. Field Crop Res. 30, 1–11.
Sinclair, T.R., Marrou, H., Soltani, A., Vadez, V., 2014. Soybean production potential in Africa. *Global Food Sec.* 3, 31–40.
Soltani, A., Hoogenboom, G., 2007. Assessing crop management options with crop simulation models based on generated weather data. Field Crop Res. 103, 198–207.
Soltani, A., Sinclair, T.R., 2012. Modeling Physiology of Crop Development, Growth and Yield. CABI Publication (322p).
Soltani, A., Maddaha, V., Sinclair, T.R., 2013. SSM-wheat: a simulation model for wheat development, growth and yield. Int. J. Plant Prod. 7, 1735–8043.
Soltani, A., Sinclair, T.R., 2015. A comparison of four wheat models with respect to robustness and transparency: Simulation in a temperate, sub-humid environment. Field Crop Res. 175, 37–46.
Stapper, M., Harris, H.C., 1989. Assessing the productivity of wheat genotypes in a Mediterranean climate, using a crop-simulation model. Field Crop Res. 20, 129–152.
Tanner, C.B., Sinclair, T.R., 1983. Efficient water use in crop production: research or research? In: Taylor, H.M., Jordan, W.R., Sinclair, T.R. (Eds.), Limitations to Efficient Water Use in Crop Production. Am. Soc. Agron, Madison, WI, pp. 1–27.
Teulat, B., Rekika, D., Nachit, M.M., Monneveux, P., 1997. Comparative osmotic adjustments in barley and tetraploid wheats. Plant Beed. 116, 519–523.
Uppala, S., Kallberg, P., Simmons, A., Andrae, U., Da Costa Bechtold, V., Fiorino, M., et al., 2005. The ERA-40 re-analysis. Q. J. R. Meteorol. Soc. 131, 2961–3012.
Wahbi, A., Sinclair, T.R., 2005. Simulation analysis of relative yield advantage of barley and wheat in an eastern Mediterranean climate. Field Crop Res. 91, 287–296.